International Journal for Housing Science and Its Applications
Publish August 10, 2025. Volume 46, Issue 4 Pages 3614-3631

https://doi.org/10.70517/ijhsa464488a

# Modeling of long-term safety and durability assessment of offshore structures under high pressure conditions via partial differential equations

**Xingwei Chen[1,2,*] and Liangwei Liu[2]**
[1] Digital Port and Shipping Application Technology Research Center, Zhejiang Institute of Communications, Hangzhou, Zhejiang, 311112, China
[2] Navigation College, Zhejiang Institute of Communications, Hangzhou, Zhejiang, 311112, China
Corresponding authors: (e-mail: cxingwei@126.com).

**Abstract** Offshore engineering needs to face huge waves and the impact of waves on the structure, and its structural strength and safety are crucial aspects in the design of offshore engineering structures. In this paper, based on the three-dimensional potential flow theory, the theoretical model of ocean engineering structure is established by using the partial differential equation of motion in time domain, and the finite element model of semi-submersible ocean platform is constructed by combining with finite element software. The safety of the ocean engineering structure is evaluated, analyzed and calibrated on the basis of considering the environmental wave loads, current loads and wind loads. Then, based on the limit state equation of the cracked structure, the PNET method is used to calculate the failure probability of the cracked structure of the offshore engineering, and the durability assessment of the offshore engineering structure is realized in this way. In the motion response of semi-submersible offshore platform, the change trend of transverse oscillation and longitudinal oscillation motion is opposite. After the wave period increases to 30~50s, the amplitude of the vertical oscillation response tends to be about 1.5 at each wave direction angle. The response amplitude of the bow rocking motion tends to be close to zero at the wave angles of 0° and 90°. 130° is the most dangerous wave direction under the LC class sea state, and the peak tension of the mooring structure of the offshore engineering platform reaches 3252.74kN, but the safety coefficient is still higher than the threshold value of 2.58%. Solving the durability of offshore engineering structures by limit state equations can guide the inspection and repair of offshore engineering structures. Relying on the time-domain partial differential equation of motion combined with finite element software can realize the effective analysis of motion response and limit state of offshore engineering structures, which can help to improve the safety and durability of offshore engineering structures in high-pressure environment.

**Index Terms** three-dimensional potential flow theory, offshore structures, time-domain motion, partial differential equations, environmental loads

## I. Introduction

At present, China's economy has developed into an export-oriented economy highly dependent on the sea, and its dependence on marine resources and space has increased significantly, and its maritime rights and interests outside its jurisdictional waters need to be constantly maintained and expanded [1], [2]. Strengthening the research related to the safety of marine engineering is of great significance to ensure safe production and promote the development process of China's ocean power. As the total number of offshore projects and their service age grows, it is increasingly important to ensure the safe operation of offshore projects and improve their resilience to disasters [3], [4]. The service environment and the loads suffered by marine engineering (such as fatigue, corrosion, erosion) are often very complex, and its service cycle is filled with a large number of disaster-causing These need to be ensured by building a strong marine country [5], [6].

The structure of marine engineering structures is complex and expensive, and once a breakage accident occurs, it will cause huge casualties and economic losses at the same time, it will also produce incalculable harm to the marine environment [7]. Therefore, no matter from the economic aspect or from the environmental safety aspect, it is crucial to ensure its safety during the service period. For marine engineering structures, while studying the fatigue problem, the rotting candle problem must be considered [8]. According to statistics, the annual loss of rotting candles in China accounts for about one percent of the gross national product, and the loss of marine rotting candles accounts for about one percent of the total loss of rotting candles [9]. Although ships and marine engineering structures are equipped with strict decay protection system at the beginning of construction, theoretically the hull decay is within the acceptable range. According to the real ship inspection, the corrosion protection system is not

effective enough during the service period of the ship, especially in some localized areas, due to aging of the coating or other factors leading to the peeling off of the coating, which will lead to more serious corrosion [10], [11]. According to the statistics, nearly of the failure of marine engineering structures is triggered by rot candles, and the fatigue of rot candles accounts for nearly of the total number of accidents. Thus, it can be seen that the fatigue of rotting candles is common and harmful in the field of marine engineering [12].

Compared with land-based engineering structures, one of the special characteristics of ships and offshore engineering structures is that they have been in the marine environment for a long time, and the surface of the structure is subjected to extremely serious corrosion [13]. Marine engineering structures will be subjected to the combined effect of alternating loads and corrosive candle environment during the service period, which makes its service time significantly shorter [14]. It is generally believed that the phenomenon of early failure of engineering structures or components due to cracking or fracture under the combined effect of alternating loads and corrosive environment is called corrosion fatigue. In the process of rot candle fatigue, there are two basic forms of damage, one is fatigue damage caused by the alternating load, and the other is rot candle damage caused by the rot candle medium [15], [16]. When the marine engineering structure suffers from the joint action of the alternating load and the corrosive environment, the role of these two types of damage is not a simple superposition, but the two basic injuries between the existence of obvious symmetry effect, that is, to promote each other's corrosive fatigue is the essence of the electrochemical corrosive candle of seawater of the steel used in marine engineering and the synergistic effect of alternating load on the mechanical damage process of the engineering structure. Therefore, the rot candles fatigue damage of marine engineering structure under the combined effect of alternating load and corrosive environment is a more serious form of rot candles mechanical damage [17], [18].

The article proposes a finite element model for offshore engineering structures based on partial differential equations, and evaluates the safety and durability of offshore engineering structures by modeling and analyzing the variation of their structural ultimate strength.

Complex finite element analyses are usually performed in offshore engineering to assess the stability, safety and durability of structures. In this paper, in order to realize the effective assessment of the safety of the offshore engineering structure, the theoretical model of the motion response of the offshore engineering structure is established by combining the three-dimensional potential flow theory and the time-domain partial differential equation of motion based on the consideration of the environmental loads. Then the simulation model of semi-submersible offshore platform is established with different units such as Shell180, Beam185, Link181 and Mass20 in ANSYS software, and after setting the coordinate system and boundary conditions, the simulation analysis is carried out for the motion response of semi-submersible offshore platform, the time-domain motion, and the safety calibration under the extreme sea state. Based on the limit state equation of the cracked structure of the offshore engineering, the PNET method is used to solve the failure probability of the cracked structure, and the structural durability index is updated based on the obtained durability, which in turn ensures the operational durability of the offshore engineering structure.

## II. Theoretical foundations of offshore structural assessment models

Marine engineering structure is mainly used in steel structure, based on the objective point of view analysis, in the long-term high-pressure environment, the limit hardness of its structure is in a high state. If the ultimate hardness is reached, brittle crack damage will easily occur, and even produce major safety accidents. Therefore, it is necessary to construct an appropriate assessment model to study the ultimate strength of the marine engineering structure, and its extreme degree is a non-linear evolutionary process, to use simulation to find out the place where the extreme strength damage is most likely to occur, and then optimize the design of this place to improve the overall strength of the marine engineering structure, and to fully ensure the safety and durability of the marine engineering structure.

### *II. A. Methods for calculating environmental loads*

#### II. A. 1) Wave loads

Calculation of the distribution of the first-order dynamic pressure of the fluid in contact with the water surface of the floating body based on the potential flow theory can be obtained:

$$p=-\rho\left(\frac{\partial\Phi(X,t)}{\partial t}\right)=i\omega\rho\varphi(X)e^{-i\omega t} \tag{1}$$

where $\rho$ is the density of the wave, $\Phi$ is the velocity potential, and $t$ is the time of action.

The first order hydrodynamic force of the floating body is:

$$Fe^{-i\omega t}=-\int_{S_0}pndS=\left[-i\omega\rho\int_{S_0}\varphi(X)ndS\right]e^{-i\omega t} \tag{2}$$

where $n$ is the unit vector perpendicular to the surface of the object, oriented from the floating body towards the fluid, and $S$ is the mean wet surface of the object, which refers to the area of the part of the object in contact with the water [19].

The wave force is divided into three parts, the first part is the Froude-Krilov force, which is related to the effect of the incident wave on the floating body, and the second part is the diffraction or bypassing force, which in general, the floating body has little effect on the wave action. The third part is the radiative force, which is obtained when a floating body in a fluid is vibrated by the action of a wave, which in turn generates its own response causing a reverse action on the fluid in contact:

$$F = F_I + F_D + F_R = -\left[ i\omega\rho\int_S \varphi_I(X)ndS + i\omega\rho\int_S \varphi_D(X)ndS + i\omega\rho\int_S \varphi_R(X)ndS \right] \tag{3}$$

where $F_I$ is the $F-K$ force, $F_D$ is the bypassing force, and $F_R$ is the radiation force.

The $F_R$ force can be disassembled into two parts containing the additional mass and the radiation damping, i.e:

$$F_R = \omega^2 A + i\omega B \tag{4}$$

where $A$ is the additional mass and $B$ is the radiation damping.

#### II. A. 2) Current loads

The flexible tube microelement under water flow is subjected to inertia force, drag force and lift force. The inertial force is expressed as:

$$F_m = \rho V_0 a + \rho C_m V_R a_r \tag{5}$$

where $F_m$ is the inertial force perpendicular to the axis of the microelement, $C_m$ is the three-dimensional additional mass coefficient, $a$ is the acceleration of the fluid point perpendicular to the axis of the linear unit, $a_r$ is the acceleration of the fluid point along the axis of the linear unit, $V_0$ is the volume per unit length, and $V_R$ is the hydrodynamic response of the volume with respect to the effect of the additional mass [20].

The resistance and $C_d$ are calculated as follows:

$$F_D = \frac{1}{2}\rho C_D a_n |a_n| D \tag{6}$$

$$C_d = \begin{cases} \frac{8\pi}{\mathrm{Re}\cdot s}\left(1-0.87s^{-2}\right), 0<\mathrm{Re}<1 \\ 1.45+8.55\,\mathrm{Re}^{-0.9}, 1<\mathrm{Re}<30 \\ 1.1+4\,\mathrm{Re}\,e^{-0.9}, 30<\mathrm{Re}<2.33\times10^5 \\ -3.41\times10^{-6}\left(\mathrm{Re}-5.78\times10^5\right), 2.33\times10^5<\mathrm{Re}<4.92\times10^5 \\ 0.401\left(1-e^{-\mathrm{Re}\left(55.99\times10^5\right)}\right), 4.92\times10^5<\mathrm{Re}<10^7 \\ s=-0.077215655+In(8/\mathrm{Re}) \end{cases} \tag{7}$$

where $F_D$ is the drag force perpendicular to the cell, $Re$ is the Reynolds number, $C_d$ is the drag coefficient, and $a_n$ is the acceleration of the fluid point along the cell normal.

The lift force is generated by the vortex flow around the flexible tube micro element and is expressed as:

$$F_L = \frac{1}{2}\rho C_L v_r^2 D \tag{8}$$

where $C_L$ is the lift coefficient.

#### II. A. 3) Wind loads

Wind load is an important environmental load that needs to be considered for ocean engineering structures under high-pressure conditions, and the calculation of wind load should start from the simulation of the wind field and the mechanism of the load. For the design and analysis of marine engineering structures, the hourly average wind speed at a height of 10m above the sea surface is generally used with time-varying components to describe the effect of wind on marine engineering structures from the energy point of view in the form of wind spectra. According to the API RP2SK specification, the commonly used NPD wind spectrum gradually replaces the API wind spectrum as the recommended wind spectrum to characterize the pulsating wind. In this paper, considering the sensitivity of different reference wind speeds, the NPD spectrum is used in the subsequent calculations of pulsating wind loads.

The NPD wind spectrum can be expressed as:

$$S(f)=\frac{320\left(\frac{u_{10}}{10}\right)^{2}\cdot\left(\frac{z}{10}\right)^{0.45}}{\left[1+1.5f_{m}\right]^{5/3n}} \tag{9}$$

$$f_{m}=172f\left(\frac{u_{10}}{10}\right)^{-0.75}\cdot\left(\frac{z}{10}\right)^{0.67} \tag{10}$$

where, $f$ is the wind speed pulsation frequency, $z$ is the vertical height from sea level, $n=0.468$, $u_{10}$ is the one-hour average wind speed at 10m above sea level.

In this paper, the wind load simulation for the offshore structure is performed by calling the Fortran-compiled 5MW wind turbine horizontal thrust and moment versus incident relative wind speed from the Userforce dynamic link library in AQWA to load the external wind load onto the offshore structure at each time step. Based on the wind force-wind speed data of the 5MW wind turbine given by NREL, the polynomial function fitting method is used to generate a continuous wind force-wind speed fitting function, and the wind force-wind speed function plot is obtained.

The horizontal thrust of the 5MW wind turbine as a function of incident relative wind speed is:

$$F=\begin{cases}-0.1241v^{4}+2.836v^{3}-16.72v^{2}+75.66v-85.06 & 3\le v<11.4\\ 0.0354v^{4}-2.801v^{3}+83.58v^{2}-1128v-6193 & 11.4\le v<24\\ -259.9v+6518 & 24\le v<25\\ 16.72v^{2}+75.66v-85.06 & v\ge 25\end{cases} \tag{11}$$

where, $F$ is the horizontal thrust applied to the wind turbine and $x$ is the incident relative wind speed.

For the over-water foundation part and tower exposed in the marine environment, the wind load on the over-water part of the structure is calculated as:

$$F_{wind}=\frac{1}{2}\rho C_{wind}Av^{2}\cos\beta \tag{12}$$

$$C_{wind}=C_{h}C_{s} \tag{13}$$

Among them, $\rho$ is the air density, $C_{wind}$ is the wind force coefficient, $A$ is the windward area of the water part, $v$ is the relative wind speed, $\beta$ is the angle between the wind direction and the $x$-axis direction. $C_{h}$ is the height coefficient of the wind component above the water surface, $C_{s}$ is the shape coefficient of the wind component above the water surface, the value of which is selected according to the shape of the component based on the specification, and 0.50 is selected for the tower and the upper floating tube.

### *II. B.Potential flow theory and time-domain equations of motion*

#### II. B. 1) Three-dimensional potential flow theory

In the hydrodynamic calculation of offshore platform structures, the Morision equation is generally used for smaller diameter objects, and the winding theory (potential flow theory) is generally used for larger structures. Since the semi-submersible offshore platform floats, columns, decks, etc. are large-size components, the hydrodynamic performance of the offshore platform structure is calculated using the potential flow theory [21]. Therefore, the corresponding velocity potential is composed of the incident wave velocity potential and scattered wave potential together, i.e.:

$$\phi=\phi_{L}+\phi_{D} \tag{14}$$

where $\bar{\phi}_{L}$ is the incident wave velocity potential and $\phi_{D}$ is the scattered wave potential generated by the structure.

The assumed fluids in the three-dimensional potential flow theory are all ideal fluids, and therefore, the fluids satisfy the Laplace equation:

$$\nabla^{2}\phi=0 \tag{15}$$

For a non-stationary fluid, the fluid satisfies the Bernoulli equation:

$$\frac{\partial\phi}{\partial t}+\frac{1}{2}(\nabla\phi)\cdot(\nabla\phi)+\frac{p}{\rho}+gz=0 \tag{16}$$

The above three equations show that only the velocity potential function of the flow field is required, which can be brought into Bernoulli's equation to find the pressure distribution of the flow field, and then the integration of the wet surface area of the platform is used to find the buoyant body force. However, the velocity potential has to satisfy the boundary conditions and initial conditions in addition to the Laplace equation.

The seafloor boundary conditions are:

$$\frac{\partial \phi}{\partial n} = 0, z = -d \tag{17}$$

Initial conditions are:

$$\begin{aligned} &\frac{\partial \phi}{\partial n} = v_n(x, y, z, 0), On\ the\ object\ surface \\ &\phi(x, y, z, 0) = f(x, y, z), On\ the\ free\ water\ surface \\ &\frac{\partial \phi}{\partial t}(x, y, z, 0) = h(x, y, z), On\ the\ free\ water\ surface \end{aligned} \tag{18}$$

**II. B. 2) Equations of motion in the time domain**

When analyzing the motion of offshore structures in waves, frequency domain or time domain differential equations of motion are usually used for the solution, but since the frequency domain differential equations of motion take into account the influence of nonlinear dynamic response and coupling effects, the motion response of offshore structures obtained by its solution may have errors. Therefore, in order to accurately calculate the dynamic response of semi-submersible offshore platforms, this paper chooses to use the time-domain differential equation of motion to solve the motion response of the platform to realize the safety analysis [22]. The motion of semi-submersible offshore platforms is usually affected by the loads generated by the four parts of wind, wave and current as well as the mooring system, and the coupling of multiple loads makes the motion of semi-submersible offshore platforms present nonlinear characteristics, in which the wind load mainly comes from the ambient aerodynamic loads, and the wave loads mainly act on the platform.

The wind load is usually defaulted to the aerodynamic load generated by the upper wind turbine. The wind turbine aerodynamic loads are firstly solved according to the foliation momentum theory, and the matrix distribution of wind load values is obtained. Subsequently, the loads are imported into the floating wind turbine whole machine coupling model to realize the coupling of multiple loads.

The wave load calculation is based on the potential flow theory as well as the frequency domain analytical solution obtained from Morrison's equation calculation. The impulse response function is obtained by transforming the linear and quadratic transfer functions through Fourier transform, and the time-domain wave load is obtained according to the wave height. For a floating platform with a suspended chain line mooring, the wave loads to be considered are mainly categorized into first-order wave forces, mean drift forces, and second-order differential frequency wave forces. The time-domain wave loads for the simple harmonic wave case are expressed as follows:

$$F_j(t) = \mathrm{Re}\left\{F_j^{(1)} e^{i\omega t}\right\} + \bar{F}_j^{(2)} + \mathrm{Re}\left\{F_j^{(2)} e^{i\omega t}\right\} \tag{19}$$

When the second-order velocity potential and the second-order wave force are considered in the time domain, the dynamical system with waves as input and the motion response of the floating platform as output of the dynamical system is no longer a linear system, and the convolution relation between the wave force in the time domain and the wave force transfer function in the frequency domain proposed by Cummins is utilized to represent the time course of the wave force by the form of convolution integral of the impulse response function and the wave surface lifting.

The instantaneous wave force acting on a floating body under the action of random waves can be written as by noting the instantaneous height of the wave surface at the floating body as $\eta(t)$:

$$F_j^{(1)}(t) = \int_0^t H_j^{(1)}(t-\tau)\eta(\tau)d\tau \tag{20}$$

$$F_j^{(2)}(t) = \int_0^t \int_0^t H_{2j}^{(2)}(t-\tau_1, t-\tau_2)\eta(\tau_1)\eta(\tau_2)d\tau_1 d\tau_2 \tag{21}$$

where $H_j^{(1)}(\tau)$ and $H_{2j}^{(2)}(\tau_1, \tau_2)$ are the impulse response functions of the first-order and second-order wave forces on the $j$ rd motion degree of freedom, respectively.

By Fourier transforming the first-order and second-order wave force transfer functions obtained from the frequency domain analysis, the first-order and second-order impulse response functions of the wave force in the time domain can be obtained. Namely:

$$H_j^{(1)}(t) = \mathrm{Re}\left\{\frac{1}{\pi}\int_0^\infty T_j^{(1)}(\omega)e^{i\omega x}d\omega\right\} \tag{22}$$

$$H_j^{(2)}(t) = \mathrm{Re}\left\{\frac{1}{2\pi^2}\int_0^\infty \int_0^\infty T_j^{(2)}(\omega_1, \omega_2)e^{i(\omega_1 R_1 + \omega_2 z_2)}d\omega_1\omega_2\right\} \tag{23}$$

where $T_j^{(1)}(\omega)$ and $T_j^{(2)}(\omega_1, \omega_2)$ are the first-order and second-order wave force transfer functions on the $j$ th degree of freedom of motion in the frequency domain, respectively.

Compared with the above two kinds of loads, the flow load of the floating platform is composed of flow force and flow moment, including longitudinal force $F_{cx}$, transverse force $F_{cy}$ and flow moment around the vertical center axis of the platform $M_{cz}$. In the time domain calculation process, the flow load needs to take into account the drag force generated by the superposition of the velocity of the flow and the horizontal velocity of the wave plasma point, and the expression is as follows:

$$F_{cx} = \frac{1}{2}\rho_a C_{cx} v_{cur}^2 TL_{cur} \tag{24}$$

$$F_{cy} = \frac{1}{2}\rho_a C_{cy} v_{cur}^2 TL_{cur} \tag{25}$$

$$M_{cz} = \frac{1}{2}\rho_a C_{cz} v_{cur}^2 TL_{cur}^2 \tag{26}$$

The mooring load part is directly solved by the mooring calculation theory, and finally the time-domain equations of motion of the floating body are organized as follows:

$$\begin{aligned} &\left[M + m(\infty)\right]\ddot{x}(t) + \int_{-\infty}^{t}\left[R(t-\tau)\right]\dot{x}(t)\,d\tau \\ &+ D_1\dot{x}(t) + D_2 f(\dot{x}) + Kx(t) \\ &= F_{win} + F_{wav} + F_{cur} + F_{cat} \end{aligned} \tag{27}$$

where $M$ is the platform $6\times6$ inertia matrix, $m(\infty)$ is the additional mass matrix at frequency infinity, $R(t)$ represents the time delay function of the memory effect of the free liquid surface, $D_1$ is the linear damping matrix including wave drift damping, $D_2$ is the second order damping matrix, and $f$ is the vector function. $K$ is the $6\times6$ hydrostatic recovery matrix, $x(t)$ is the platform $6\times1$ motion vector, $F_{win}$ the wind load vector, $F_{wav}$ is the wave load vector, $F_{cut}$ is the current load vector, and $F_{cat}$ is the recovery force provided by the external, mooring system.

## III. Finite element modeling of offshore structures

Wind analysis and wind load calculations in offshore engineering can be utilized for offshore structural safety assessment and structural design to ensure safety under strong winds. Offshore engineering often needs to consider the fatigue effects of factors such as tides, waves and currents on structures as a way to enhance the durability of offshore structures under high pressure conditions. Complex finite element analyses are often performed to assess the stability and strength of structures. Based on the stability and ultimate strength analysis of marine engineering structures, thus better clarifying the safety performance of marine engineering structures, providing reliable technical support to ensure the safe operation of marine engineering, and continuously improving the reliability and safety of marine engineering.

### *III. A. Finite element modeling of offshore structures*

#### III. A. 1) Finite element analysis methods

When analyzing and studying the ultimate strength of semi-submersible offshore engineering structure, it can be found that the structure of semi-submersible offshore engineering is a gradual destruction process, according to the support of the finite element theory to build the model of semi-submersible offshore engineering, and the incremental curvature method of structural damage to calculate and analyze, it can be found that the curve of structural stress change of semi-submersible offshore engineering, and the change of buckling of the steel structure with the change of yielding has a certain connection,. Therefore, when studying the ultimate strength of steel structure, the change of buckling effect can be generalized to the scope of data analysis.

After calculating by nonlinear finite element analysis, it can be found that the disturbance change of unit plasticity and the change of unit average force is a strain relationship, in order to improve the accuracy of the calculation, it can be improved by the accuracy of the unit average force - average strain force, and such a finite element analysis method is known as step-by-step damage analysis method.

In the calculation of ultimate strength analysis of semi-submersible marine engineering, the direct calculation method of finite element can be adopted. In other words, the ultimate strength is estimated according to the deformation amount of the cross-section plastic moment of the semi-submersible offshore engineering and the ultimate deformation amount of the longitudinal bottom plate of the hull. In order to reduce the influence of structural bearing capacity on the change of structural ultimate strength during the estimation, the structural stress carried by the reinforcing bar unit is not taken into account when estimating the structural ultimate strength of the semi-submersible offshore project. Because in the early stage of ultimate strength, the load stress of reinforcement will

be reduced appropriately, and the load stress area will be redistributed. Therefore, if the load data information of reinforcing bars is referred to in the estimation, the value of the ultimate strength of the steel structure will be increased, which will bring some influence to the subsequent research and analysis.

### III. A. 2) Finite element model structure

In this paper, based on the recommendations on the semi-submersible offshore platform model in the recommended practice for column-stabilized platforms of the Det Norske Veritas (DNV), ANSYS software is used to establish an integrated finite element model of the main body of the target offshore platform and the mooring system, and the specific results are shown in Fig. 1. Among them, according to the form and force characteristics of each component, different cell types such as Shell180, Beam185, Link181, Mass20, etc. in ANSYS software are selected respectively.

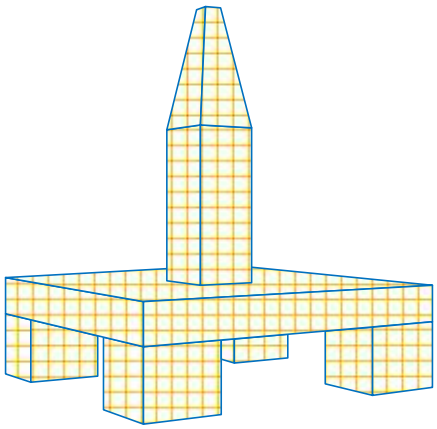

Figure 1: Marine platform finite element model

(1) The Shell180 cell is a shell cell that can be used to model relatively thin shell forms. The four nodes at the corners of the cell can either move translationally along the XYZ direction of the nodal coordinate system or rotate around the XYZ axis, so each point has six degrees of freedom. When simulating thin films, the nodes can be set to have only translational degrees of freedom. When its degenerate triangles option is activated, the mesh generation applies only to filled cells. In this paper, the main structure of the semi-submersible platform is simulated with Shell180 cells.

(2) Beam185 cell is a beam cell, based on the theory of Timuchenko beam structure, and taking into account the factor of shear deformation, it can be used to simulate beams with moderate or large slenderness ratios. Beam185 is a three-dimensional beam cell with two nodes, I and J, and each of them has six to seven degrees of freedom, which can be translated along the XYZ direction and rotated around the XYZ axis, and the introduction of cross-section warping as the seventh degree of freedom can also be considered. Warping of the cross-section can also be considered as the seventh degree of freedom. In this paper, the Beam185 unit is used to simulate the upper towering tower of the semi-submersible platform.

(3) Link181 unit is a three-dimensional rod unit, which can only withstand axial tension and pressure, and nodes I and J each have three degrees of freedom, i.e., translational along the XYZ direction of the coordinate system. The unit can meet the elasticity, plastic hardening, large deformation, large strain, as well as adjusting the unit life and death and other functional requirements, through the setting of attributes can be realized only by the tensile or only by the pressure. In this paper, Link181 unit is used to simulate the anchor chain of semi-submersible platform.

(4) Mass210 unit is defined based on a single point element, which can simulate counterweight and ballast, the unit has six degrees of freedom, and can move along the XYZ coordinates and rotate around the XYZ axis, and can be given a specific mass and moment of inertia in any direction. In this paper, the Mass20 cell is used to simulate the counterweight and ballast of a semi-submersible platform.

### III. A. 3) Coordinate system and boundary conditions

There are two coordinate systems in AQWA, the global coordinate system and the following coordinate system. The global coordinate system is fixed, and its coordinate origin is the intersection of the centerline of the semi-submersible platform and the waterline surface, the XOY surface is coincident with the still water surface, and the Z-axis is coincident with the centerline of the semi-submersible platform and is perpendicular to the upward surface of the still water surface. The following coordinate system is fixed on the semi-submersible platform and moves with the movement of the semi-submersible platform, and its coordinate origin is located in the center of gravity of the

semi-submersible platform. When the semi-submersible platform is stationary, the direction of its three axes is consistent with that of the global coordinate system and follows the right-hand rule. At the same time, it is stipulated that the wave angle is 0° when the wave propagates along the X-axis of the global coordinate system, and 90° when the wave propagates along the Y-axis of the global coordinate system, and the wave angle increases with the counterclockwise change of the wave.

Define the spatial right-angle coordinate system O-XYZ for the computational model in this paper, as shown in Fig. 2, the XOY plane coincides with the hydrostatic water surface, and the structure in this coordinate system has six degrees of freedom, three degrees of freedom of movement and three degrees of freedom of rotation, i.e., degrees of freedom of movement along the X direction: longitudinal oscillation (Surge), degrees of freedom of movement along the Y direction: transverse oscillation (Sway), and degrees of freedom of movement along the Z direction: Heave, and degrees of freedom of rotation around the X direction: Roll, around the Y direction: Pitch, and around the Z direction: Yaw, with the positive direction obeying the right-handed spiral rule.

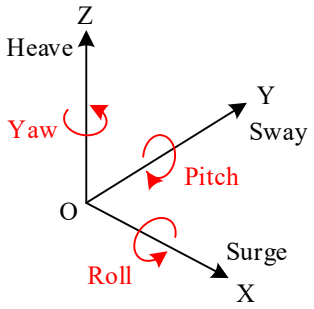


Figure 2: Coordinate and six degrees of freedom

In the motion response analysis of the semi-submersible platform foundation, only the wave frequency motion of the semi-submersible platform foundation under the action of waves is considered in the analysis because the semi-submersible platform foundation is not equipped with a mooring system. When setting the environmental parameters, the water depth is set to 220 m, the wave frequency range is 0.1-2.5 rad/s, and the step frequency number is 25. The wave angle range is 0-90°, the interval is 20°, and the number of wave angles is eight. Meanwhile, NPD spectrum and constant wind are used in the calculation process.

### *III. B. Calculation of durability of offshore structures*

#### III. B. 1) Limit state equations for structures

The cut-off point for assessing whether a structure is in a normal functional state or in a state of failure is the limit state, which is a sign of whether the structure is in a reliable working state. When the structure is not strong enough to resist the external loads within the expected time limit, the structure is in a state of failure, while the opposite is true for the structure. The ultimate limit state of load carrying capacity for structural analysis is the final limit state of the structure, including yield damage, buckling damage, institutional plastic damage, fatigue damage and cracking damage. The limit state of normal use of the structure corresponds to the serviceability limit state, including local damage failure, super-deformation failure and structural vibration failure of the components, which will not directly lead to the overall structural damage and failure, but in order to ensure the safety of the structure, the structural design should try to avoid such limit states [23].

Describing the various types of random factors affecting the durability analysis of structures can be expressed as a set of random variables called the functional function of the structure. Namely:

$$X = \left[ X_1 \quad X_2 \quad \cdots \quad X_n \right] \tag{28}$$

The structural limit state function expressed in terms of random variables is:

$$Z = g\left( X_1 \quad X_2 \quad \cdots \quad X_n \right) \tag{29}$$

where $Z$ is the safety margin of the structure and when $Z = 0$, it is determined as the failure surface of the structure. The expression for the safety margin is:

$$Z = g\left( S, R \right) = R - S \tag{30}$$

where $R$ is the resistance of the structure and $S$ is the external load on the structure. When $Z > 0$, it represents that the structure's own resistance is greater than the external load effect on the structure, and the structure is in a durable state. When $Z = 0$, it represents that the structure's own resistance is equal to the external load effect on

the structure, and the structure is in the limit load state. When $Z<0$, it means that the resistance of the structure itself is less than the external load effect on the structure, and the structure is in the failure state.

The common indicators for measuring the durability of structures are durability $P_r$ and probability of failure $P_f$, with durability $P_r$ representing the probability that the structure will fulfill its intended function at a predetermined time and under predetermined conditions, and probability of failure $P_f$ being the probability that the structure will fail to fulfill its intended function. It can be expressed by the following formula:

$$\begin{aligned} P_r &= P\left[Z=R-S>0\right] \\ P_f &= P\left[Z=R-S<0\right] \\ P_r &+ P_f = 1 \end{aligned} \tag{31}$$

$$f_z(z)=\frac{1}{\sqrt{2\pi}\sigma_z}\exp\left[-\frac{(Z-\mu_z)^2}{2{\sigma_z}^2}\right] \tag{32}$$

where $\mu_Z=\mu_R-\mu_S$, $\sigma_Z=\sqrt{{\sigma_R}^2+{\sigma_S}^2}\mu_z$, $\mu_R$, $\mu_S$ are the mean value of $Z$, $R$, $S$, $\sigma_Z$, $\sigma_R$, $\sigma_S$ are the standard deviation of $Z$, $R$, $S$ respectively.

According to the expression of safety margin state of the structure, when $Z<0$, the structure is in the failure state, and the failure probability can be expressed as:

$$\begin{aligned} P_f &= \int_{-\infty}^{0} f_z(Z)dZ = F_z(0) \\ &= \int_{-\infty}^{0}\frac{1}{\sqrt{2\pi}\sigma_z}\exp\left[-\frac{(Z-\mu_z)^2}{2{\sigma_z}^2}\right]dz \end{aligned} \tag{33}$$

Durability is expressed as:

$$\begin{aligned} P_r &= \int_{-\infty}^{0} f_z(z)dz \\ &= \int_{0}^{\infty}\frac{1}{\sqrt{2\pi}\sigma_z}\exp\left[-\frac{(Z-\mu_z)^2}{2\sigma_z^2}\right]dz \end{aligned} \tag{34}$$

The variables are standardized to be normalized and the standardized normal variable is denoted as $u$:

$$u=\frac{Z-\mu_z}{\sigma_z} \tag{35}$$

When $Z=-\infty$, $u=-\infty$; when $Z=0$, $u=-u_z/\sigma_z$. The failure probability can be expressed as:

$$P_f=\int_{-\infty}^{\frac{\mu_z}{\sigma_z}}\frac{1}{\sqrt{2\pi}}\exp\left[-\frac{u^2}{2}\right]du \tag{36}$$

$$P_f=\int_{\frac{\mu_z}{\sigma_z}}^{\infty}\frac{1}{\sqrt{2\pi}}\exp\left[-\frac{u^2}{2}\right]du \tag{37}$$

Order $\beta=\frac{\mu_z}{\sigma_z}$, known as the durability index of the structure, is a measure of the durability of the structure.

**III. B. 2) Calculation of structural durability**

The PNET method is the application of probabilistic network estimation techniques to structural system reliability analysis. The method considers that structural failure modes can be categorized into primary and secondary failure modes, and then $G$ representative failure modes are selected from the primary failure modes. The principle of selecting a representative failure mode is to group the major failure modes, and each major failure mode in the same group is highly correlated with a representative failure mode, which is the one with the highest probability of failure among all the failure modes in the group. From the correlation condition, it is known that it can approximately represent the failure probability of all failure modes in the group. It is assumed that the representative failure modes in different groups are independent of each other.

Thus, if the failure probability of the $j$ rd major failure mode among the $G$ representative failure modes is $P_{fj}$, the failure probability of the structural system is:

$$P_{fi} = 1 - \prod_{j=1}^{G} \left(1 - P_{fj}\right) \tag{38}$$

The basic steps for calculating the probability of structural failure by the PNET method are as follows:

Step1 List the main failure modes $E_k$, and the corresponding functional functions $Z_k$ ($k = 1, 2, \cdots, I$, the number of main failure modes), and find out the durability index $\beta_k$ of the corresponding $Z_k$. Sort each $E_k$ according to its $\beta_k$ value from the smallest to the largest, and use the obtained serial number as the basis of the order of the failure modes. The sequence of major failure modes is $E_k\left(k = 1, 2, \cdots, I\right)$.

Step2 Take the major failure mode $E_1$ with the smallest durability index as a representative failure mode. Calculate the correlation coefficient $\rho_{i1}\left(i = 2, 3, \cdots, I\right)$ between each other major failure mode and this representative mode $E_1$. A value of $\rho_0$ ($\rho_0$ called the partition correlation coefficient) is selected as the basis for determining the degree of correlation between each major failure mode and this representative failure mode $E_1$. When $\rho_{i1} \geq \rho_0$, it is considered that the primary failure mode $E_i$ can be replaced by the representative failure mode $E_1$, i.e., the primary failure mode $E_i$ can be disregarded. Otherwise, when $\rho_{i1} \leq \rho_0$, the primary failure mode $E_i$ and the representative failure mode $E_1$ are considered statistically independent of each other. In this way, all $\rho_n > \rho_0$ major failure modes are grouped together, with $E_1$ as their representative. This group of primary failure modes is considered to be highly correlated with $E_1$, and assuming that they are perfectly correlated (i.e., the correlation coefficient is 1), the probability of failure of $E_1$ is used $P_f$ as the probability of failure of this group of primary failure modes.

Step3 From the remaining failure modes, find out the one with the smallest reliability index as the second representative failure mode, according to the method of Step2, find out the main failure mode it represents, and take them as a new group of main failure modes, assuming that they are completely correlated, and take the failure probability of the second representative failure mode as the probability of failure of this group of failure modes. Repeat the above steps until the major failure modes are all grouped.

Step4 Take these representative modes and calculate the failure probability of the structural system.

## IV. Safety and durability assessment of offshore structures

Semi-submersible offshore engineering platform, as a platform with more applications in marine resources exploration and development, is prone to fatigue under high-pressure conditions such as wind, waves, currents and other environmental loads as well as operational dynamic loads during offshore operations, which seriously threatens the safe and reliable operation of the platform. Once an accident occurs, it will cause huge losses. Therefore, it is of great significance to carry out the long-term safety and durability assessment and analysis of semi-submersible offshore platforms under high-pressure conditions to ensure the safe and stable operation of offshore engineering structures.

### *IV. A. Safety assessment of offshore structures*

#### IV. A. 1) Motion response of semi-submersible platforms

In order to study the influence of different wave directions and wave periods on the motion response of the semi-submersible offshore engineering platform, with reference to the DNV specification and considering that the structure is symmetric about the Y-axis and the X-axis, the range of the wave direction from 0 to 90° is selected, with the step size of 20°, and a total of 8 wave angles, and the range of the wave period is from 1 to 50s, with the interval of 1s, and a total of 50 periods. Using the semi-submersible offshore engineering platform model designed in this paper, the model simulation is carried out by finite element simulation software, and the motion response of the semi-submersible offshore engineering platform is obtained as shown in Fig. 3, in which Fig. 3(a)~(b) shows the motion response amplitude distribution of longitudinal and transverse waves, respectively.

From Fig. 3(a), it can be seen that the trends of the longitudinal oscillatory motion with period at different wave direction angles are similar. The overall trend of longitudinal oscillatory motion response is increasing in the whole range of wave period. Under the same period, the smaller the wave direction angle, the larger the amplitude of the motion response. The amplitude of the longitudinal oscillatory motion response reaches the maximum when the period is 50s and the wave direction angle is 0°. When the wave angle is 90°, the amplitude of the longitudinal motion response is the smallest, and the overall tendency is close to zero, which is a reasonable trend.

In Fig. 3(b), at different wave direction angles, the transverse oscillatory motion shows an increasing trend with the change of wave period. At the same wave period, the response amplitude of the transverse oscillatory motion

increases as the wave direction angle increases. The response amplitude of the transverse oscillatory motion is largest when the wave period is 50 s and the wave direction angle is 90°, and reaches a minimum when the wave direction angle is 0°. In contrast, the trend of longitudinal oscillatory motion is similar to that of transverse oscillatory motion, with an overall decreasing trend. Under the same wave period, the response amplitude of longitudinal oscillatory motion gradually decreases with the increase of wave direction angle. The response amplitude of the longitudinal motion is largest when the wave period is 50 s and the wave angle is 0°, and reaches the minimum when the wave angle is 90°. In general, the transverse oscillatory motion has an opposite trend to the longitudinal motion.

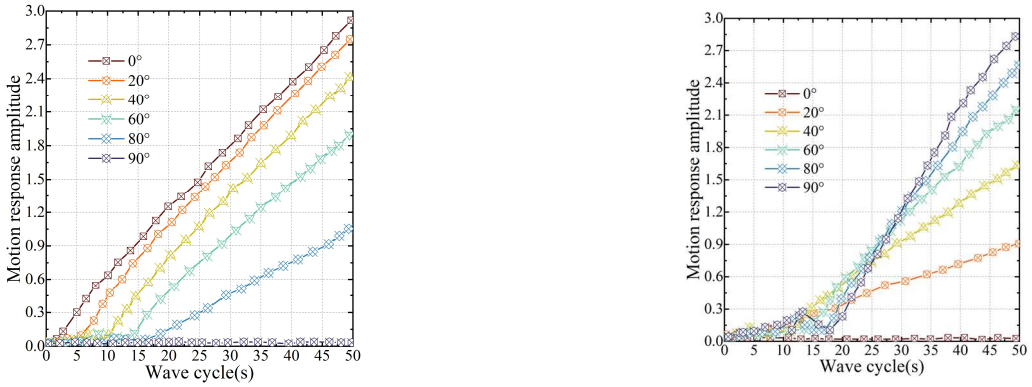


(a) Surge response amplitude (b) Sway response amplitude

Figure 3: Semi-submersible platform movement response

Fig. 4(a)~(b) shows the response amplitude of pendulum and longitudinal rocking motions of the semi-submersible offshore engineering platform, respectively. The overall pendulum motion shows a similar trend when the period changes. When the period is 15.5s, the droop response amplitude changes dramatically, decreasing sharply from 7.5s to 15.5s and increasing sharply from 15.5s to 17.5s. The amplitude of the droop response reaches its maximum at a period of 15.5s and a wave direction angle of 40°. As the period increases to 30~50s, the amplitude of the droop response tends to be around 1.5 for each wave angle. At different wave angles, the longitudinal oscillatory motion tends to increase with the change of wave period, especially in the wave period of 0-15s, the amplitude of the longitudinal oscillatory motion response changes drastically. After the wave period exceeds 20s, the amplitude of the longitudinal motion response generally shows a decreasing trend. When the wave period is 5s and the wave angle is 0°, the amplitude of the longitudinal rocking response reaches the maximum value, and reaches the minimum value of 0 when the wave angle is 90°.

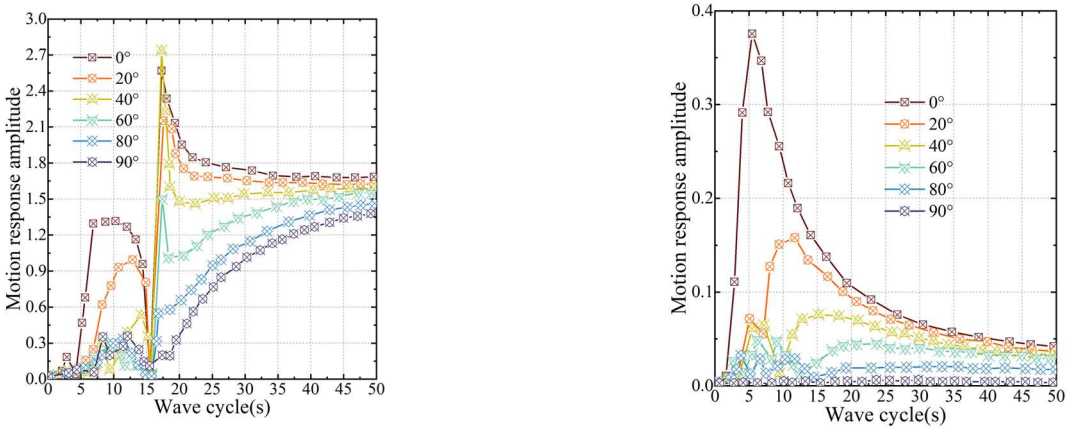


(a) Heave response amplitude (b) Roll response amplitude

Figure 4: Semi-submersible platform movement response

Figure 5(a)~(b) shows the amplitude of the transverse and bow rocking motion response of the semi-submersible offshore engineering platform, respectively. As can be seen from the figures, the transverse rocking motion response curves have similar trends at different wave angles. In the wave period of 0s-15s, the amplitude of the transverse rocking motion response shows a large fluctuation phenomenon, and the change trend is obvious. Between 15s and 17s, the response amplitude increases with the wave period, and the upward trend is obvious. After 17s, the response amplitude shows a decreasing trend with the change of wave period. When the wave period is 17s and the wave direction angle is 60°, the response amplitude of transverse rocking motion reaches the maximum. When the wave direction angle is 0°, the response amplitude is minimized and tends to zero, which is opposite to the case of longitudinal rocking motion. The bow rocking motion response curve has no obvious pattern about wave direction, and the motion response amplitude generally shows an increasing trend in the whole wave period interval. Between the wave period of 0s-10s, the amplitude of the bow rocking motion response shows a small fluctuation. When the wave period is 50s and the wave angle is 60°, the amplitude of the bow rocking motion response is the largest. At 0° and 90°, the amplitude of the motion response is small, and the overall value tends to be close to zero.

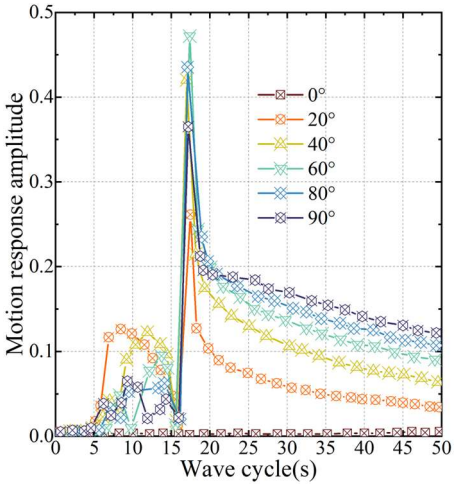


(a) Pitch response amplitude

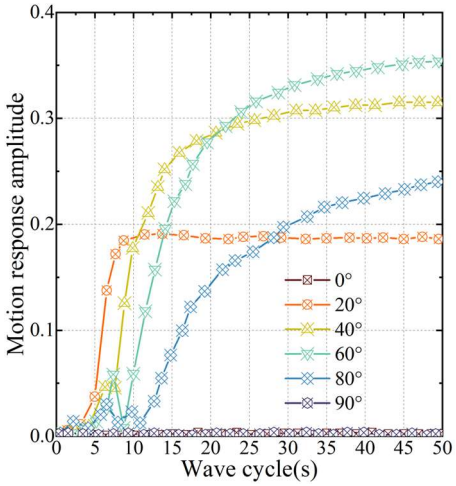


(b) Yaw response amplitude

Figure 5: Semi-submersible platform movement response

**IV. A. 2) Joint time-domain analysis of wind and wave currents**

Semi-submersible offshore platforms are subject to a variety of environmental loads under normal operating conditions, such as wind, waves, currents and other common sea loads. In order to better investigate the environmental adaptability of the semi-submersible offshore platform, three different structures (three floats (TRI), four floats (FBT) and two floats (TFT)) of semi-submersible offshore platforms are compared with each other under the environmental conditions of multiple loads, which is a way to better carry out the design of offshore structures. In the finite element simulation software, the wave heights are adopted as the common wave heights in each season, and the JONSWAP spectrum is irregular with a peak factor of 3.5. Table 1 shows the definition of working conditions for various environmental conditions. The NPD wind spectrum is used, the average wind speed in 1h is 11.5m/s, the sea surface current velocity is used 0.8m/s, and the directions of wind, wave and current are all in 0º direction. The effects of irregular waves of JONSWAP spectra with different working conditions and different spectral peak periods on the motion response of various semi-submersible offshore platforms under the combined effect of wind, wave and current are considered.

Table 1: Definition of working conditions for various environmental conditions

| - | | I | II | III |
|---|---|---|---|---|
| NPD wind spectrum<br>Average wind winds (m/s) | | 11.5 | 11.5 | 11.5 |
| JONSWAP | Righteous wave (m) | 2.8 | 2.8 | 2.8 |
| | Peak cycle (s) | 6 | 12 | 18 |
| | Peak factor | 3.5 | 3.5 | 3.5 |
| Flow Surface velocity (m/s) | | 0.8 | 0.8 | 0.8 |

Table 2 shows the statistical results of the motion amplitude of different semi-submersible offshore platforms under the combined action of wind and wave currents at different working conditions, where the sign of the maximum value represents the direction only, and responds to the displacement response value when the absolute value of the motion is the largest.

Considering the maximum motion response results of the three semi-submersible offshore engineering platforms under the combined action of wind and wave currents at different spectral peak period wave conditions, it is shown that the maximum value of the motion response of the three-float wind turbine platform in the Ⅰ, Ⅱ, and Ⅲ conditions is the largest compared to the other wind turbine bases in the degrees of freedom of transverse rocking, bow rocking, longitudinal swinging as well as transverse swinging, followed by four-float, while two-float cabin type has the smallest value. In the pendulum direction, the maximum value of the motion response of the three types is not large, the three-float and four-float types are between 1.25 and 1.57 m. The pendulum amplitude of the two types is close to that of the two-float type, and the two-float type has the largest value under each working condition. Under the longitudinal swinging freedom, the movement angle of three-float type is the smallest in all Ⅲ working conditions, the four-float type is the smallest in other working conditions, and the two-float compartment type is the largest in all working conditions. Since the action directions of wind, wave and current are all in the direction of 0° with the X-axis, the maximum values of the three motion response amplitudes are more obvious in longitudinal oscillation and longitudinal rocking.

Table 2: Different semi-submersible sea platform sports amplitude

| Degree | Type | Max value | | | Mean value | | |
|---|---|---|---|---|---|---|---|
| | | TRI | FBT | TFT | TRI | FBT | TFT |
| Surge (m) | Ⅰ | 27.42 | 22.43 | 16.53 | 16.39 | 13.74 | 8.51 |
| | Ⅱ | 28.59 | 22.06 | 14.72 | 15.84 | 13.15 | 8.04 |
| | Ⅲ | 29.14 | 22.18 | 15.89 | 16.18 | 12.38 | 7.87 |
| Sway (m) | Ⅰ | 17.53 | 3.68 | 0.15 | 0.72 | -0.02 | 0.00 |
| | Ⅱ | 16.28 | 7.25 | 0.18 | 0.51 | 0.05 | 0.02 |
| | Ⅲ | 13.24 | 7.43 | 0.37 | 0.15 | 0.05 | 0.02 |
| Heave (m) | Ⅰ | -1.25 | -1.26 | -2.21 | -0.85 | -0.88 | -1.42 |
| | Ⅱ | -1.37 | -1.31 | -2.55 | -0.82 | -0.85 | -1.43 |
| | Ⅲ | -1.56 | -1.57 | -3.38 | -0.82 | -0.82 | -1.45 |
| Roll (°) | Ⅰ | 2.63 | 0.38 | 0.06 | 0.11 | 0.01 | 0.01 |
| | Ⅱ | 2.37 | 0.74 | 0.08 | 0.09 | 0.01 | 0.01 |
| | Ⅲ | 2.15 | 0.82 | 0.14 | 0.05 | 0.01 | 0.01 |
| Pitch (°) | Ⅰ | -2.34 | -2.18 | -3.41 | -1.12 | -1.15 | -1.83 |
| | Ⅱ | -2.52 | -2.31 | -4.72 | -1.18 | -1.12 | -1.75 |
| | Ⅲ | -2.93 | -3.09 | -4.38 | -1.23 | -1.03 | -1.69 |
| Yaw (°) | Ⅰ | 20.95 | 1.46 | 0.43 | 0.86 | 0.02 | 0.03 |
| | Ⅱ | 18.72 | 3.35 | 0.46 | 0.62 | 0.08 | 0.07 |
| | Ⅲ | 16.47 | 3.51 | 0.87 | 0.31 | 0.05 | 0.09 |

**IV. A. 3) Safety calibration for extreme sea states**

In order to further verify the safety performance of the offshore engineering structure under different sea conditions, the surface current velocity is set to 0.95m/s, the 1h average wind speed is 36.5m/s, the meaningful wave height is 15.5m, the spectral peak period is set to 18s, and the spectral peak factor is 3.6 in the finite element software, which is named as the LC class sea condition. Based on the environmental conditions of LC-level sea state, the mooring structure of the semi-submersible offshore platform is analyzed by time-domain coupled dynamic analysis under the main dangerous wave direction, and the top tension of the mooring cable and the lifting force of the anchor end of the semi-submersible offshore platform are safety-checked under the LC-level sea state, so as to verify the structural safety of the semi-submersible offshore platform meeting the extreme sea state and to provide support for the design of the offshore engineering structure.

In the assessment of the extreme sea state, the maximum value of the dynamic response of the mooring structure of the semi-submersible offshore platform is statistically analyzed by the maximum response average method, which has a high confidence level and forecasting efficiency. In order to provide sufficient data for the statistical analysis, in the time-domain coupled dynamic calculation of the full wave direction, six different wave random numbers with

a duration of 5 hours are calculated for each wave direction, and 50 working conditions are calculated for the complete state of the mooring structure of the semi-submersible offshore engineering platform to ensure the accuracy of the safety assessment.

The mooring cable tension and the vertical lifting force on the anchor end calculated by applying the maximum response average method to six different wave random numbers under each wave direction in the intact state are counted, and the specific results are shown in Fig. 6. Among them, Fig. 6(a) shows the top tension of the mooring cable with the maximum force in each wave direction under LC class sea state, and Fig. 6(b) shows the safety factor of the mooring cable with the maximum force in each wave direction and the lifting force on the anchor end.

The dynamics of the mooring structure of the semi-submersible offshore engineering platform in the intact state is analyzed under the LC class sea state, and the following conclusions are obtained:

(1) By comparing the maximum tension in the mooring structure of the semi-submersible offshore engineering platform in the complete state of each wave, it is found that the most dangerous wave direction in the LC sea state is 130°, and the peak tension in the mooring structure of the lower semi-submersible offshore engineering platform is 3252.74kN, and the safety factor reaches a minimum of 1.59, but it is still greater than the minimum allowable safety factor of 1.55, which passes the safety check. And the peak value of tension is very close to the safety threshold value of mooring cable tension 3304.51, and only 51.77kN is reserved, which accounts for 1.57% of the safety threshold value of tension. It shows that the environmental conditions under LC class sea state are very close to the limit sea state that the mooring structure of the complete state semi-submersible offshore engineering platform can carry, and also verifies the correctness of the preliminary determination of LC class sea state as the limit sea state.

(2) The maximum value of the anchor lifting force also occurs in the 130° wave direction, reaching 9.04*10-6N, which is much smaller than the safety threshold of the anchor lifting force of 50N, and successfully passes the safety check.The anchor lifting force in the other wave directions other than the 130° wave direction shows a relatively uniform trend, which is significantly lower than that of the anchor lifting force in the 130° wave direction. However, since the magnitude of the anchor end lifting force is negligible, the mooring cable of the semi-submersible offshore engineering platform has almost no upward dialing effect on the anchor foundation in the LC class sea state.

(3) Under the LC class sea state, the maximum value, average value and standard deviation of the tension in the mooring cable with the highest tension in the mooring structure of the semi-submersible offshore engineering platform can still show a relatively uniform trend under the initial sea state, which indicates that the designed mooring structure of the semi-submersible offshore engineering platform has a good adaptability and stability to the environmental conditions of different classes.

(4) The main dangerous wave directions in LC class are 20°, 50°, 70°, 130° and 160°, and the safety coefficients are 1.65, 1.67, 1.73, 1.59 and 1.71, respectively. The dangerous wave directions in the time-domain coupled dynamics calculations with different random numbers of waves in the full-wave downward direction are in agreement with the results of the dangerous wave direction search before the determination of the limit sea state, which verifies the correctness of the preliminary process of determining the limit sea state. The correctness of the preliminary determination process of the limit sea state is verified.

In conclusion, under the LC class sea state, the maximum tension and the lifting force of the mooring structure of the complete semi-submersible offshore platform can pass the safety check, and the maximum tension and the safety threshold of the mooring cable tension are very close to each other, with a small margin of allowance, and the environmental conditions under the LC class sea state are very close to the limit sea state that the complete mooring system can carry, and the results obtained at this time can be regarded as The results obtained at this time can be regarded as the maximum conditions that the marine engineering structure can withstand. Therefore, the design of offshore engineering structures based on the environmental parameters at this time can effectively ensure the safety of offshore engineering structures under high-pressure conditions.


(a) The top tension of the max mooring line

(b) Safety factor and Anchor lift

Figure 6: The safety check of the extreme sea condition

## *IV. B. Durability assessment of offshore structures*

### IV. B. 1) Calculation of durability of engineering structures

Fatigue crack extension in offshore structures under high pressure conditions is a complex problem influenced by a large number of factors, most of which are fundamentally random. For the reinforced plate members containing initial cracks in the offshore engineering structure, the inherent uncertainties in the geometry of the cracks, the material parameters and the loading parameters will lead to the fatigue performance of the reinforced plate members showing obvious uncertainties, which will have an impact on the reliability of the overall structure of the offshore engineering. Therefore, when carrying out the durability calibration of the offshore engineering structure, it is necessary to adopt the durability analysis method to carry out a scientific and reasonable assessment of the offshore engineering structure.

Based on the semi-submersible offshore engineering platform established in this paper, the crack size of the structure under different conditions is simulated in finite element software. Because the crack size will gradually increase with the accumulation of time, the strength of the offshore engineering structure decreases, and the overall durability will be gradually reduced. The crack extension size distribution and critical crack size of different reinforced plates on the profile of semi-submersible offshore platforms calculated by the crack extension probability model under different phase differences are brought into the limit state equations, and the fatigue durability indexes and corresponding structural durability or failure probability of each reinforced plate can be obtained according to the PNET method.

Due to the limitation of space, the calculation results of the reinforced plates in representative positions in the structure of semi-submersible offshore engineering platforms are taken as an example, which are the No. 6 and No. 159 reinforced plates located farther away from the neutralization axis at the deck and the bottom plate of the platform, respectively. The variation of structural durability of the reinforced plate with time under different phases is shown in Fig. 7, in which Figs. 7(a)~(d) show the structural durability of the No. 6 and No. 159 reinforced plates with the belt plate and the web plate, respectively.

Observing the structural durability calculation results of the two typical locations of the reinforced plates, it can be seen that the structural durability of the No. 6 reinforced plate located at the deck is the lowest, and the durability of its belt plate and web plate is 97.43% and 92.07%, respectively. The durability of the reinforcing plate located at the bottom of the platform is better, and the durability of the reinforcing plate web is significantly lower than that of the reinforcing plate belt plate. In addition, observing the effects of different phases on the structural durability of the reinforced plate, it can be seen that for the No. 6 reinforced plate of the platform deck, which is mainly subjected to tensile loads, the difference in durability under different phase differences is small. Analyzing from the perspective of probability and durability, the longer the crack extension length of the reinforced plate, the weaker the structural strength of the reinforced plate, the lower and lower the durability of the structure, and the greater the possibility of failure. Therefore, these reinforced plate components, which are located at the deck and bottom plate of the semi-submersible offshore platform and away from the neutral and axial positions, which are subjected to large loads, should be paid attention to in the process of structural safety inspection, and structural repair should be carried out in a timely manner to ensure the use of the durability of the semi-submersible offshore platform.

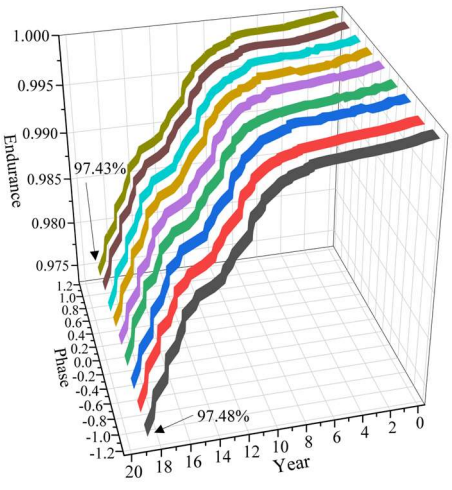


(a) Reinforced plate strap-6

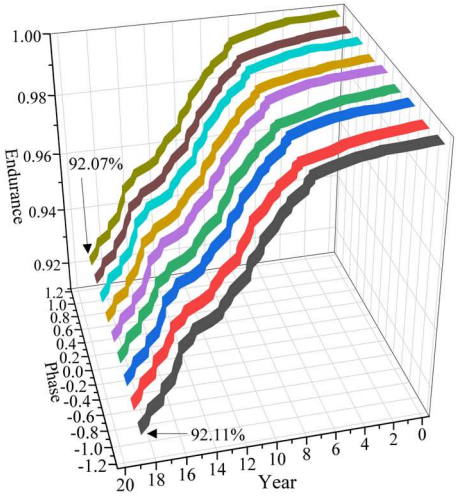


(b) Reinforced plate abdominal-6

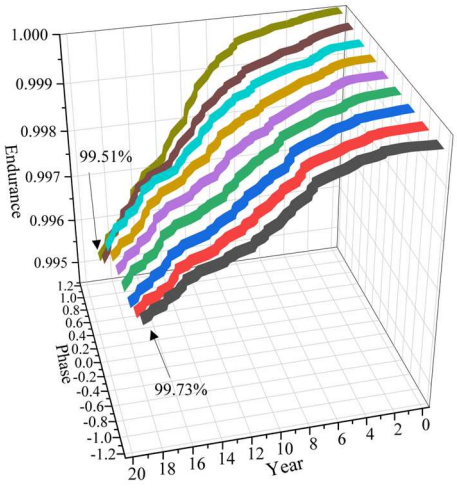


(c) Reinforced plate strap-159

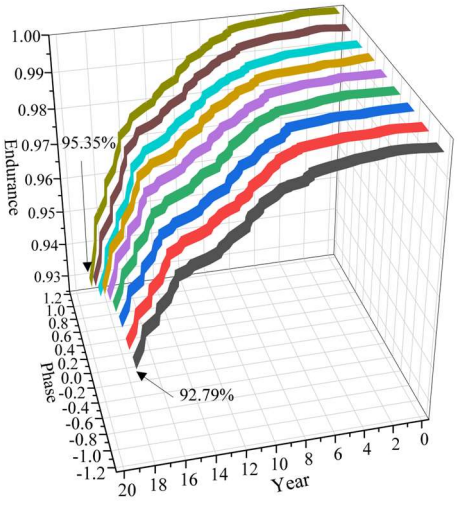


(d) Reinforced plate abdominal-159

Figure 7: The change of structural durability at any time

**IV. B. 2) Structural durability update analysis**

In order to ensure the safety and reliability of offshore structures throughout the period of operation, it is important to keep track of the performance of the hull structure and to control the expansion of cracks. Under normal circumstances, the aging process of a structure can be effectively controlled by regular overhaul. Structural overhaul programs and maintenance based on the durability assessment method can reduce costs during the service life of an offshore project, and by setting inspection and repair intervals based on the risk of possible damage rather than on arbitrary cycles, the method can also reduce repair costs and downtime. The durability of an offshore project can be improved by calculating the probability of failure of each important part of the offshore project. The crack extension probability model of cracked reinforced plate established in the previous paper can be used to find the durability index of the structure over time, which can be used to guide the inspection and maintenance during the service period of the ocean engineering.

For the cracked reinforced plate structure of the semi-submersible offshore platform in this paper, the durability of the structure can be updated based on the inspection results. The probability of failure of the reinforced plate structure is derived by the PNET method, where the minimum detected crack size of 10 mm is taken as an illustration. The probability of failure of the structure after the first inspection where no cracks are detected can be derived from the PNET method. Subsequent updates can be repeated until the end of the service life. In this way, an inspection program can be established that meets the durability requirements of the structure. Based on the results of the previous calculations of durability and assuming that the inspection interval is 5 years, the durability index update of the structure is shown in Fig. 8. Where Fig. 8(a)~(b) shows the durability indices of the unrepaired as well as the inspected and repaired structure at 5-year intervals, respectively.

The inspection reveals that when the durability index of the structure is lower than the required target value, the structure is required to be repaired. If the structure is treated with repair, its performance is restored to the initial state. Assuming that the target reliability index is 2.7 (i.e., 99.95% durability), the cracked reinforced plate structure of the semi-submersible offshore platform designed in the paper is required to be repaired if the durability index of the structure has fallen below the target value by the 5th year. Through inspection and repair, the change of the reliability index of the structure always stays above the durability index requirement of the semi-submersible offshore platform. By solving the durability failure probability of the offshore engineering structure and then obtaining its durability change, adopting the inspection and repair maintenance method can ensure that the failure probability of the offshore engineering structure is always lower than the target value, so as to enable it to carry out the offshore engineering activities in a safer way and to improve the operational durability of the offshore engineering structure.

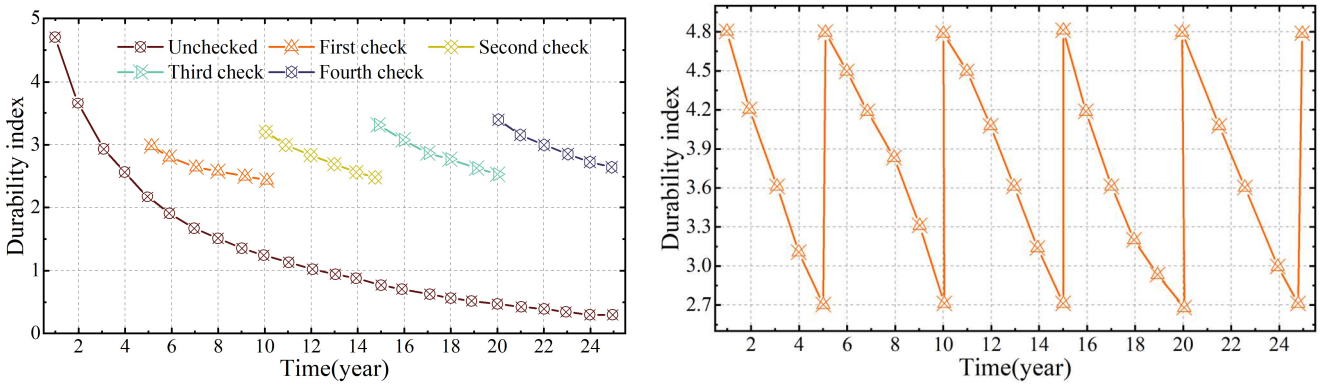


(a) Check and No repair for every five years

(b) Check and repair for every five years

Figure 8: The durability index of the structure is updated

## V. Conclusion

In the article, a finite element model of semi-submersible offshore platform is established by introducing time-domain differential equations of motion and finite element software on the basis of considering the environmental loads, which is combined with the structural limit state equations to calculate the durability of offshore engineering structures. In the motion response of the semi-submersible ocean platform, the amplitude of the droop response at each wave direction angle tends to be about 1.5 as the period increases to 30~50s later. In the wave period between 0s-10s, the amplitude of bow rocking motion response shows a small fluctuation phenomenon.The most dangerous wave direction under LC class sea state is 130°, and the peak tension value of 3252.74kN appears in the mooring structure of semi-submersible ocean engineering platform under this wave, and the safety coefficient reaches the minimum of 1.59, but it is still higher than the safety threshold value of 2.58%. Based on the cracked structure of the reinforced plate of the offshore engineering, combining the structural limit state equation and the PNET method can realize the failure probability calculation of the cracked structure, so as to obtain the durability of the offshore engineering structure. Based on the durability, the inspection and repair of the durability of marine engineering structure can better ensure the timely detection and repair of the cracked structure of marine engineering and improve the durability of marine engineering structure.

## Funding

The second batch of Zhejiang Province "14th Five-Year Plan" teaching reform projects of higher vocational education: “Research and practice on the integration path of science, education, and innovation of higher vocational navigation technology specialty group under the background of world-class strong port” (Project No.: jg20240063).

High-level talent introduction project of Zhejiang Institute of Communications, “Research on durability deterioration of reinforced concrete square piles in the marine environment” (Project No.: 2024rcxm07).

## References

[1] El-Reedy, M. A. (2019). Offshore structures: design, construction and maintenance. Gulf Professional Publishing.

[2] Zhang, Y., Kim, C. W., & Tee, K. F. (2017). Maintenance management of offshore structures using Markov process model with random transition probabilities. Structure and Infrastructure Engineering, 13(8), 1068-1080.

[3] Ma, K. T., Luo, Y., Kwan, C. T. T., & Wu, Y. (2019). Mooring system engineering for offshore structures. Gulf Professional Publishing.

[4] Jimenez-Martinez, M. (2020). Fatigue of offshore structures: A review of statistical fatigue damage assessment for stochastic loadings. International Journal of Fatigue, 132, 105327.

[5] Randolph, M., & Gourvenec, S. (2017). Offshore geotechnical engineering. CRC press.

[6] Guédé, F. (2019). Risk-based structural integrity management for offshore jacket platforms. Marine Structures, 63, 444-461.

[7] Dehghani, A., & Aslani, F. (2019, August). A review on defects in steel offshore structures and developed strengthening techniques. In Structures (Vol. 20, pp. 635-657). Elsevier.

[8] Yang, S., Meng, D., Guo, Y., Nie, P., & Jesus, A. M. D. (2023). A reliability-based design and optimization strategy using a novel MPP searching method for maritime engineering structures. International Journal of Structural Integrity, 14(5), 809-826.

[9] Wang, P., Tian, X., Peng, T., & Luo, Y. (2018). A review of the state-of-the-art developments in the field monitoring of offshore structures. Ocean Engineering, 147, 148-164.

[10] Luo-Theilen, X., & Rung, T. (2019). Numerical analysis of the installation procedures of offshore structures. Ocean engineering, 179, 116-127.

[11] Moan, T. (2018). Life cycle structural integrity management of offshore structures. Structure and Infrastructure Engineering, 14(7), 911-927.

[12] Mukhtasor, M., Junianto, S., & Prastianto, R. W. (2018). On Offshore Engineering Rules for Designing Floating Structure of Tidal Current Energy Conversion System. Applied Mechanics and Materials, 874, 71-77.

[13] van Es, S., Slot, H., Steenbergen, H., Maljaars, J., & Pijpers, R. (2018). Use of HSS and VHSS in steel structures in civil and offshore engineering: Requirements regarding material properties. Steel Construction, 11(4), 249-256.
[14] Meng, D., Hu, Z., Wu, P., Zhu, S. P., Correia, J. A., & De Jesus, A. M. (2020, June). Reliability-based optimisation for offshore structures using saddlepoint approximation. In Proceedings of the Institution of Civil Engineers-Maritime Engineering (Vol. 173, No. 2, pp. 33-42). Thomas Telford Ltd.
[15] Tian, X., Wang, Q., Liu, G., Liu, Y., Xie, Y., & Deng, W. (2019). Topology optimization design for offshore platform jacket structure. Applied Ocean Research, 84, 38-50.
[16] Morales, L. D., Silva, G. P., Barros, L. D. O., & Malcher, L. (2023). Damage to fracture in offshore engineering materials under several stress states: Blowout preventer valve application. Advances in Structural Engineering, 26(11), 2025-2054.
[17] Kyriakides, S., & Corona, E. (2023). Mechanics of Offshore Pipelines: Volume I: Buckling and collapse. Gulf Professional Publishing.
[18] Mehmanparast, A., & Vidament, A. (2021). An accelerated corrosion-fatigue testing methodology for offshore wind applications. Engineering Structures, 240, 112414.
[19] Jun Liang,Yuhao Fu,Ying Wang & Jinping Ou. (2024). Identification of equivalent wind and wave loads for monopile-supported offshore wind turbines in operating condition. Renewable Energy(PA),121525-121525.
[20] Sarat Chandra Mohapatra,C. Guedes Soares & Kostas Belibassakis. (2024). Current Loads on a Horizontal Floating Flexible Membrane in a 3D Channel. Journal of Marine Science and Engineering(9),1583-1583.
[21] Albaev D.A. (2023). Estimation of non-linear amplitudes of ship motions based on three-dimensional potential theory. Transactions of the Krylov State Research Centre(Special issue 1).
[22] Pavosevic Fabijan,Tao Zhen,Culpitt Tanner,Zhao Luning,Li Xiaosong & Hammes-Schiffer Sharon. (2020). Frequency and Time Domain Nuclear-Electronic Orbital Equation-of-Motion Coupled Cluster Methods: Combination Bands and Electronic-Protonic Double Excitations. The journal of physical chemistry letters(15).
[23] Ahmed M. Abdelmaksoud & Fadi Oudah. (2024). A limit state approach for considering greenhouse gas emissions in the structural design of buildings: Environmental Impact Limit State (EILS). Journal of Building Engineering110866-110866.